This is an *Accepted Manuscript*, which has been through the Royal Society of Chemistry peer review process and has been accepted for publication.

Accepted Manuscripts are published online shortly after acceptance, before technical editing, formatting and proof reading. Using this free service, authors can make their results available to the community, in citable form, before we publish the edited article. We will replace this *Accepted Manuscript* with the edited and formatted *Advance Article* as soon as it is available.

You can find more information about *Accepted Manuscripts* in the **Information for Authors**.

ChemComm

Dynamic Article Links ▶

COMMUNICATION

Multiplex Plasmonic Anti-counterfeiting Security Labels Based on Surface-enhanced Raman Scattering

Yan Cui,[a] In Yee Phang,[b] Yih Hong Lee,[a] Mian Rong Lee,[a] Qi Zhang,[a] Xing Yi Ling[*a]

We demonstrate a multiplex plasmonic anti-counterfeiting platform by embedding multiple molecules on a single substrate with superior nanometer scale spectral and spatial resolution. The encoded specific molecular information can only be read out using Raman spectroscopy. Multiplexing increases the complexity of these plasmonic security labels without compromising the spectral resolution.

10 There is an urgency to develop novel anti-counterfeiting technology, because counterfeits and pirated goods pervade all levels of modern society.[1] The 2015 global economic impact of counterfeiting is forecasted to reach US$1.7 trillion, putting 2.5 million legitimate jobs at risk annually.[2] Furthermore, the number 15 of seized counterfeit goods continues to increase annually.[3] As such, smart security labels with increased complexity have to be designed to deter counterfeiting. Nanomaterials such as noble metal nanodisks,[4] fluorescent nanostructures,[5] colloidal photonic crystals,[6] magnetically assembled $Fe_3O_4@SiO_2$ colloids[7] 20 exhibiting unique properties under external stimuli such as light, heat, and magnetic field have been applied in security labeling. These new technologies are not known to the counterfeiters, making them more challenging to be forged. Another example of a smart security label is one that is equipped with "layered 25 security" technology.[8] In this type of security label, the first security level is a simple colorimetric or invisible feature made known to and easily validated by the general public. Additional covert features cana lso be embedded within this label, which can only be exclusively authenticated by advanced analytical 30 instruments. Such layered security labels offer a bonus level of protection against counterfeiting by providing additional identification information to distinguish between authentic and counterfeit products.

The combination of noble metal nanostructures with surface-35 enhanced Raman scattering (SERS) presents an ideal platform to develop layered security labels.[8, 9] The molecular fingerprints of Raman peaks are significantly narrower than fluorescence emissions, providing the basis for high spectral difference between two unique fingerprints with minimal cross-talk in 40 multiplex platforms.[10] Surface plasmons associated with metal nanostructures generate intense enhancement of local electromagnetic fields, and lead to strong SERS signals from probe molecules in the vicinity of these nanostructures.[11] We have previously made use of Ag nanowire arrays functionalized 45 with a single probe molecule as layered security labels.[8] The covert security features can be selectively read-out through x- or y-polarized SERS imaging, with these features otherwise indiscernible using normal characterization techniques. In this work, only one probe molecule was used on a homogeneous 50 platform to produce the covert security features. Such a system under-utilizes the potential complexity offered by SERS, since the database of Raman active molecules is tremendous.

Here, we develop a multiplex plasmonic anti-counterfeiting platform with superior nanometer scale spectral and spatial 55 resolution. By creating sandwich nanowire structures, we are able to embed multiple molecules on the same substrate to generate unique security features when individual vibrational modes are selected. Two platforms are demonstrated here: a homogenous platform in which the same security feature can be revealed at 60 different spectral positions, and a heterogeneous platform in which different features can be produced using different vibrational modes. Our multi-molecular approach increases the spectral complexity such that it will be extremely challenging to decode the molecular structures without prior knowledge. At the 65 same time, we are able to differentiate between two closely-spaced peaks, achieving an ultrahigh spectral difference between two unique fingerprints of ∼ 3.5 nm. No security feature is generated outside of this small spectral window.

The sandwich structure is central to our multiplex SERS anti-70 counterfeiting strategy because it enables multiple probe molecules to be functionalized onto our nanostructures sequentially. Nanowire structures with widths of 500 nm, lengths of 20 μm, and heights of 500 nm are first fabricated using two-photon lithography via a direct laser-writing process (Figure 1A, 75 B). These nanowires are then metallized via a thermal evaporation process with 100 nm-thick Ag. The probe molecules, 4-methylbenzenethiol (4-MBT), are functionalized onto the metalized nanowires via a ligand exchange process. After the ligand exchange, a second Ag layer is thermally evaporated over 80 the first Ag layer to generate the first sandwich structure (Ag/4-MBT/Ag). The second Ag layer enables a second probe molecule, rhodamine B isothiocyanate (RhBITC), to be functionalized onto the nanowire structures. The entire structure is metallized again to create a double sandwich structure (Figure 85 2A).
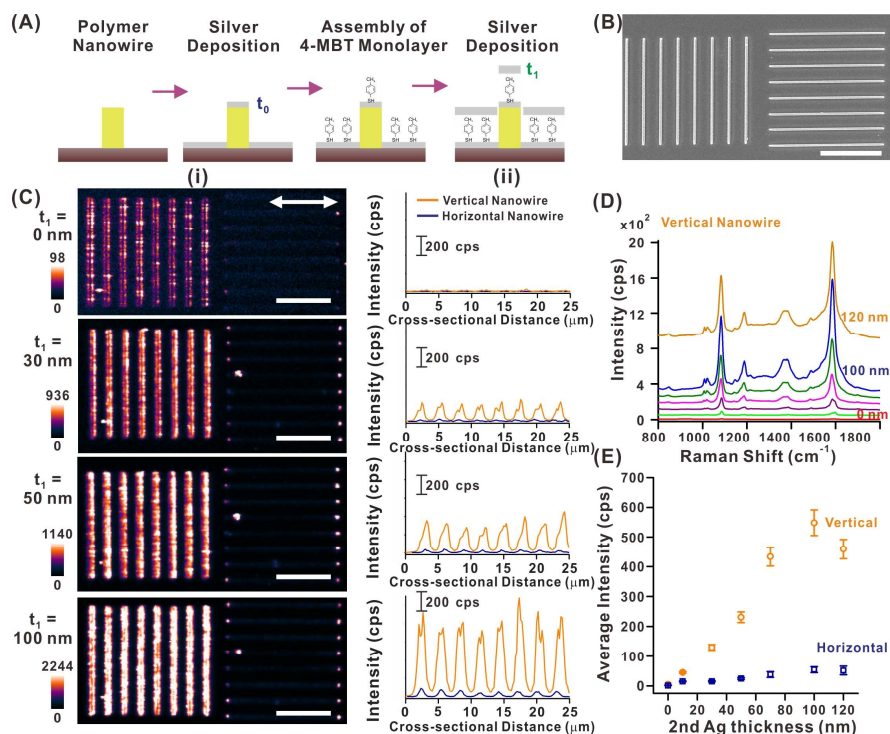
Figure 1. Optimizing the sandwich structure parameters. (A) Fabrication protocol of sandwich structure. (B) SEM image of the array of vertical and horizontal nanowires. (C) 2D SERS images (i) and SERS intensity profiles (ii) along x and y axes of line arrays, derived using the 1078 cm^{-1} vibrational mode of 4-MBT with an x-polarized incident laser excitation. The second layer of Ag coating increases from 0 nm, 10 nm, 30 nm, 50 nm, to 100 nm. All the scale bars are 10 μm, and cps stands for counts per second. (D) SERS spectra and (E) SERS intensity plot of 4-MBT from the sandwich structure at different thicknesses of second Ag layer.

The sandwich structures do not disrupt the SERS polarization-dependence of the nanowire arrays (Figure 1C-i, C-ii). Consistent with findings from our earlier research, the vertical nanowires show strong SERS response due to the excitation of the plasmon resonance at x-polarization. On the other hand, SERS intensities are weaker for the horizontal lines because of the momentum mismatch between incident photons and the propagating plasmons. Signals from the background are negligible due to the low surface roughness of the Ag film.[8]

We find that the 100 nm Ag/4-MBT/100 nm Ag layout produces the strongest 4-MBT signals. Arrays of vertical and horizontal nanowires based on 100 nm Ag/4-MBT/x nm Ag sandwich structures are constructed (Figure 1C), with x ranging from 10 nm, 30 nm, 50 nm, 70 nm, 100 nm, to 120 nm. x-y SERS images of the Ag/4-MBT/Ag sandwich structures are created using the 1078 cm^{-1} peak of 4-MBT under x-polarized excitation. SERS intensities increase with increasing thickness of the second Ag layer up to 100 nm for both the horizontal and vertical nanowire arrays (Figures 1C and E). The much stronger SERS signals from the sandwich structure also leads to a greater contrast between the nanowire structures and the background, with the nanowire morphology more clearly defined. When compared against the SERS signal without the second Ag layer coating, the SERS signals at 100 nm coating are enhanced 117-fold and 36-fold for the vertical and horizontal nanowire array, respectively. A decrease in SERS intensity is observed when the thickness of second Ag layer coating is increased to 120 nm.

The strong signal enhancement of the sandwich structure arises from the creation of additional hotspots from the deposition of the second Ag layer. The small size of 4-MBT (< 1 nm) implies that the second Ag layer is very closely spaced from the first Ag layer in our sandwich structure. Consequently, plasmon coupling between these two Ag layers leads to a strong enhancement of the local electromagnetic fields, giving rise to intense SERS

signals.[12] Furthermore, the thermal evaporation process creates nanoscale asperities on the nanowire surface and this serves to further enhance the SERS signals from the sandwich structures. The signal decrease after 100 nm coating likely arises from the creation of a smoother Ag film with lesser asperities and the obstruction of SERS signals from 4-MBT. A total of two metallization steps are required to create the double sandwich structure after 4-MBT functionalization in our experiments. As such, we limit the maximum allowable thickness of subsequent Ag layers to 100 nm such that the signals of 4-MBT do not become obscured during the metallization steps.

Next, we fabricate a layered panda double sandwich structure, where the first and second layers are homogeneously functionalized with 4-MBT and RhBITC, respectively (Figure 2A, B). This thus forms a homogeneous multiplex anti-counterfeiting platform. Both molecules have unique vibrational modes at 1078 cm^{-1} and 1200 cm^{-1}, which we use to generate the SERS images (Figures 2E and F). In the presence of a single sandwich structure with only 4-MBT present, a single SERS image of a smiling panda shows up when the 1078 cm^{-1} peak is selected (Figure 2C), but the structure is invisible at 1200 cm^{-1}. With the addition of a second RhBITC-functionalized sandwich structure, two images can be produced by selecting the 1078 cm^{-1} and 1200 cm^{-1} peaks, respectively (Figure 2D).

Our multiplex anti-counterfeiting platform offers enhanced spectral complexity as well as superior the spectral difference between two unique fingerprints, when compared against conventional colorimetric read-out techniques. The composite SERS spectrum of 4-MBT and RhBITC is more complex than their individual SERS spectra. Without the knowledge of molecule choice, it will be extremely challenging for counterfeiters to resolve the SERS spectra to deduce the number and type of probe molecules used. The second advantage relates to the narrow bandwidth of the SERS bands. 4-MBT exhibits a
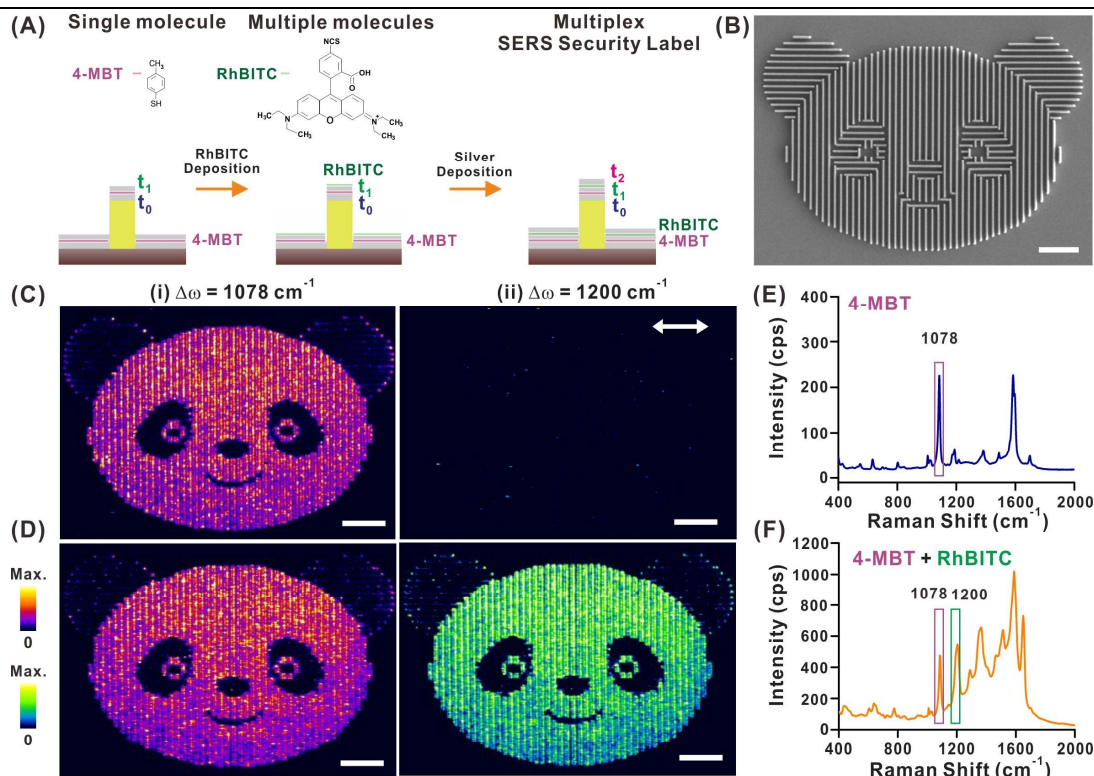
Figure 2. Homogeneous plasmonic anti-counterfeiting security labels. (A) Scheme demonstrating the construction of an Ag multiplex double sandwich structure. (B) SEM image of a panda pattern formed by arrays of vertical and horizontal nanowires. (C) x-polarized 2D SERS images created using the sandwich structure embedded with only 4-MBT, at (i) 1078 cm^{-1} and (ii) 1200 cm^{-1}. These two bands are the unique vibrational modes of 4-MBT and RhBITC respectively. In the absence of RhBITC, no SERS image can be generated at 1200 cm^{-1}. (D) x-polarized 2D SERS images created using the double sandwich structure multiplexed with 4-MBT and RhBITC, at (i) 1078 cm^{-1} and (ii) 1200 cm^{-1} band. In the presence of RhBITC, two identical images can be generated at two unique spectral positions. All scale bars are 10 μm. (E) SERS spectra of 4-MBT. (F) Composite SERS spectra of 4-MBT and RhBITC from the double sandwich structure, cps stands for counts per second.

vibrational mode at ~1078 cm^{-1}. However, selecting at 1200 cm^{-1} for the single sandwich structure in Figure 2C does not produce the panda image. It is only when an actual peak from RhBITC is present in the panda structure, that selecting the 1200 cm^{-1} peak allows the second panda image to be produced. This peak difference of 122 cm^{-1} corresponds to a mere 3.5 nm difference in spectral positions of the two vibrational modes. Such a high spectral difference gives rise to an ultrasensitive anti-counterfeiting technology that is at least 10-fold higher in resolution compared to counterfeiting technologies using quantum dots or fluorescence dyes, where their FWHM are in the range of 35 – 100 nm.[13]

To further enhance the complexity of our anti-counterfeiting platform, we create a heterogeneous multiplex platform, where individual nanostructures are encoded with their own molecular information. This leads to even better spatial resolution as compared to the homogeneous platform. We demonstrate this using the iconic Merlion symbol, comprising the Merlion itself and a gushing water stream. This first Merlion sandwich structure is created by metallization, 4-MBT functionalization, a second metallization step with 50 nm Ag (Figure 3A). This is followed by the fabrication of the gushing water stream, where the nanowires are also metallized, functionalized with secondary molecule, RhBITC, and followed by another metallization process.

The SERS image generated using the 1078 cm^{-1} peak for 4-MBT gives rise to distinct fine features of the Merlion (Figure 3B-ii), whereas its fine features are hard to distinguish in the respective SEM image (Figure 3B-i). No feature shows up at 1200 cm^{-1} after the fabrication of the first sandwich structure (Figures 3B-iii), due to the absence of RhBITC (spectrum a in Figure 3D). Furthermore, the gushing water stream is not observed at 1078 cm^{-1} even after the second sandwich structure has been fabricated (Figures 3C-ii, spectrum c in Figure 3D, E), ascertaining the integrity of our security labels. The Merlion with the gushing water stream (Figure 3C-iii) are observed at 1200 cm^{-1} for the double sandwich structure. These data successfully demonstrates the added security of our heterogeneous multiplex anti-counterfeiting SERS-based platform, with additional features showing up in a second spectral window. This is in contrast to the homogeneous platform, which generates only one pattern at two different spectral positions.

In summary, we demonstrate a multiplex SERS-based anti-counterfeiting security label using a sandwich structure. Using our Ag nanowire arrays, we are able to fabricate both homogeneous and heterogeneous sandwich structures with superior spatial resolution and the spectral difference between two unique fingerprints. Our anti-counterfeiting platform offers unique readouts that are significantly more sophisticated and secure than most colorimetric-based readout techniques. The sandwich structure enables the use of two probe molecules with non-overlapping SERS peaks to construct individual images
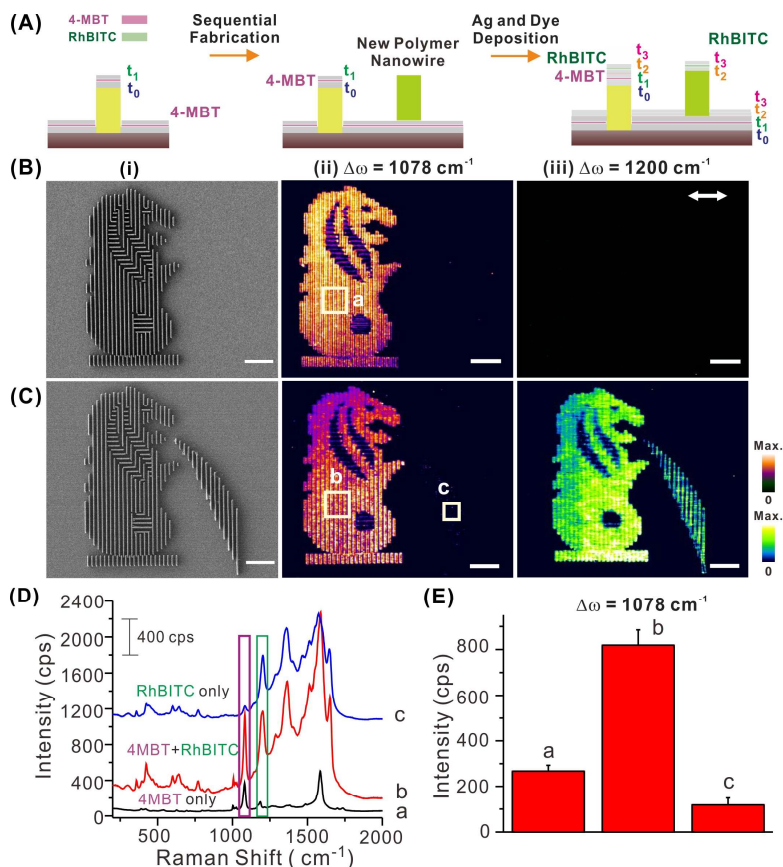
Figure 3. Heterogeneous plasmonic anti-counterfeiting security labels using the Merlion structure. (A) Scheme demonstrating the construction of a heterogeneous double sandwich structure. The Merlion figure is fabricated as the first sandwich structure, embedded with 4-MBT. The second sandwich structure (gushing water stream) is sequentially fabricated, embedded with RhBITC. (B) SEM image (i), x-polarized 2D SERS images generated at (ii) 1078 cm^{-1} and (iii) 1200 cm^{-1} demonstrates successful fabrication of this structure. (C) SEM image (i), x-polarized 2D SERS images generated at (ii) 1078 cm^{-1} and (iii) 1200 cm^{-1} show that the Merlion figure can be discerned from 4-MBT while both Merlion and the water stream can be generated using RhBITC. All scale bars are 10 μm. (D) Average SERS spectra from the selected areas labeled a, b and c in (B-ii) and (C-ii). (E) Comparison of the peak intensity of 1078 cm^{-1} band of 4-MBT from the selected areas show enhanced 4-MBT signals in the Merlion double sandwich structure but negligible signals at the gushing water stream, cps stands for counts per second.

within a homogeneous platform. Additional features can also be fabricated on the same platform using heterogeneously functionalized nanostructures, each embedded with the target probe molecule with unique molecular fingerprints. The exceptional spectral difference between two unique fingerprints of ~ 3.5 nm has yet to be demonstrated using conventional colorimetry-based optical detection techniques. The potential security and complexity of our system can further be enhanced using multiple sandwich structures with more probe molecules. Moving anti-counterfeiting platform to flexible polyethylene terephthalate (PET) substrate and using wide-field Raman 2D imaging system will enable our anti-counterfeiting label more practical in near furture.

Notes and references

a Division of Chemistry and Biological Chemistry, School of Physical and Mathematical Sciences, Nanyang Technological University, Singapore 637371.; E-mail: xyling@ntu.edu.sg
b Institute of Materials Research and Engineering, A*STAR, 3 Research Link, Singapore 117602.

1   B. Yoon, J. Lee, I. S. Park, S. Jeon and J. M. Kim, *J. Mater. Chem. C*, 2013, **1**, 2388; A. Mullard, *Nat. Med.*, 2010, **16**, 361.
2   Frontier Economics Ltd, Estimating the global economic and social impacts of counterfeiting and piracy, an executive summary commissioned by business action to stop counterfeiting and piracy (BASCAP), London, 2011.
3   K. Degardin, Y. Roggo and P. Margot, *J. Pharm. Biomed. Anal.*, 2014, **87**, 167.
4   K. Kumar, H. G. Duan, R. S. Hegde, S. C. W. Koh, J. N. Wei and J. K. W. Yang, *Nat. Nanotechnol.*, 2012, **7**, 557.
5   H. H. Pham, I. Gourevich, J. E. N. Jonkman and E. Kumacheva, *J. Mater. Chem.*, 2007, **17**, 523.
6   H. S. Lee, T. S. Shim, H. Hwang, S. M. Yang and S. H. Kim, *Chem. Mater.*, 2013, **25**, 2684.
7   R. Y. Xuan and J. P. Ge, *J. Mater. Chem.*, 2012, **22**, 367.
8   Y. Cui, R. S. Hegde, I. Y. Phang, H. K. Lee and X. Y. Ling, *Nanoscale*, 2014, **6**, 282.
9   Y. Cui, I. Y. Phang, R. S. Hegde, Y. H. Lee and X. Y. Ling, *ACS Photonics*, 2014, **1**, 631.
10 X. M. Qian, X. H. Peng, D. O. Ansari, Q. Yin-Goen, G. Z. Chen, D. M. Shin, L. Yang, A. N. Young, M. D. Wang and S. M. Nie, *Nat. Biotechnol.*, 2008, **26**, 83; T. Shegai, B. Brian, V. D. Miljkovic and M. Kall, *Acs Nano*, 2011, **5**, 2036.
11 D. L. Jeanmaire and R. P. Vanduyne, *J. Electroanal. Chem.*, 1977, **84**, 1; M. Moskovits, *Rev. Mod. Phys.*, 1985, **57**, 783.
12 H. Z. Yu, J. Zhang, H. L. Zhang and Z. F. Liu, *Langmuir*, 1999, **15**, 16; Y. Jiang, A. Wang, Z. Q. Tian and A. Otto, *J. Phys. Chem. C*, 2009, **113**, 5526; H. Y. Guo, W. Q. Xu, J. Zhou, S. P. Xu and J. R. Lombardi, *Nanotechnology*, 2013, **24**.
13 W. W. Yu, E. Chang, R. Drezek and V. L. Colvin, *Biochem. Biophys. Res. Commun.*, 2006, **348**, 781; X. Y. Cheng, S. B. Lowe, P. J. Reece and J. J. Gooding, *Chem. Soc. Rev.*, 2014, **43**, 2680.